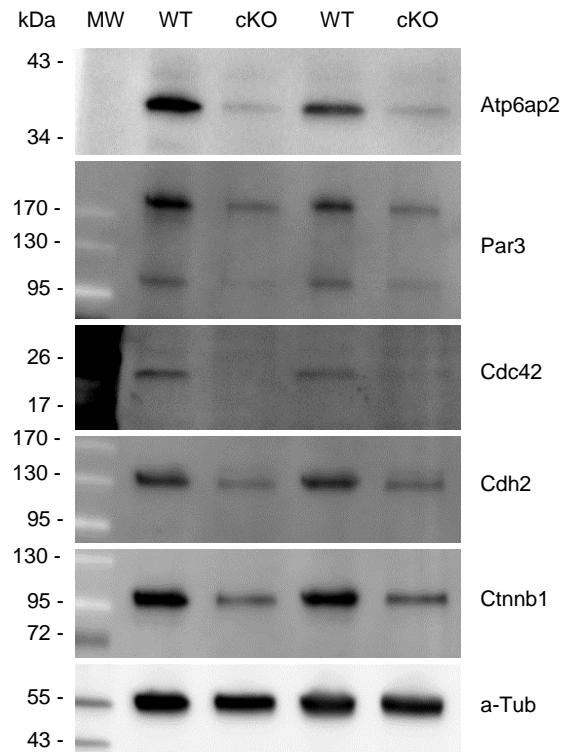
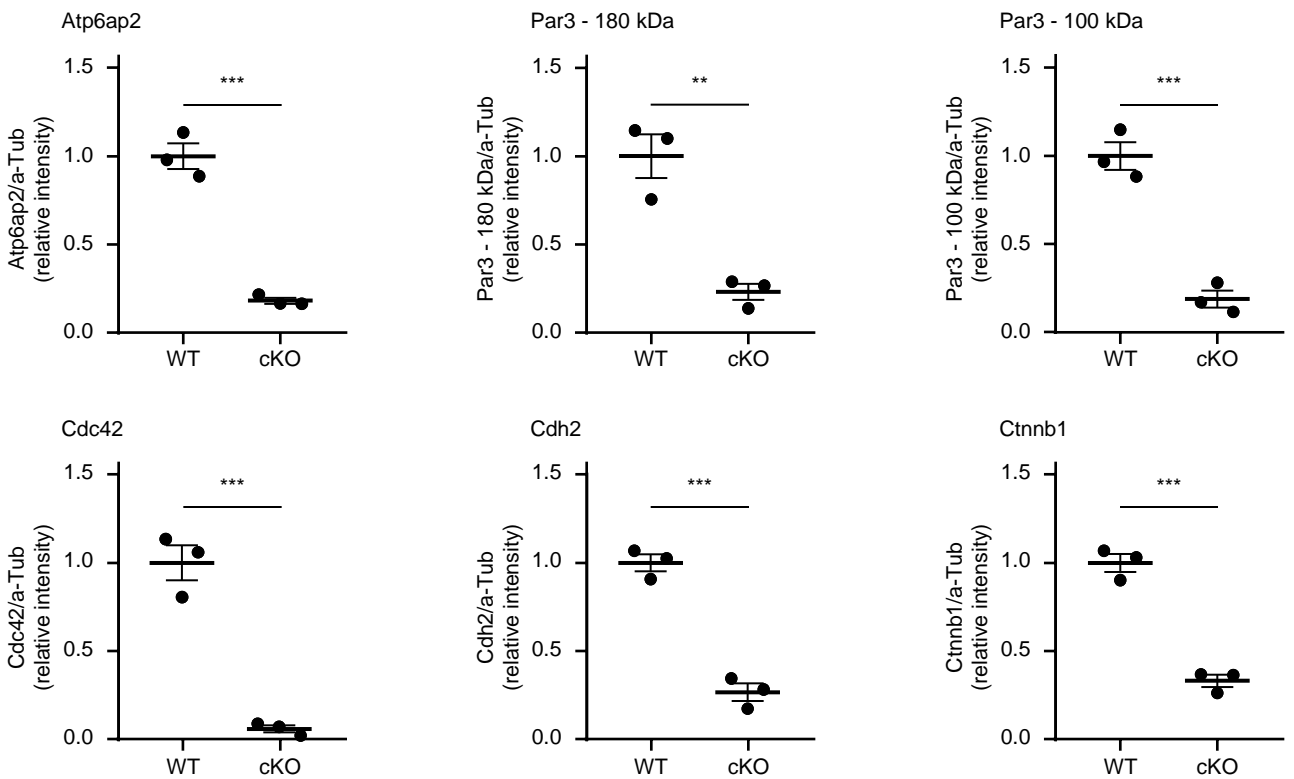


Supplemental Figure 1. *Atp6ap2* deletion in embryonic cortical stem/progenitors cells impairs self-renewal and induces cell cycle exit. (A) Staining of *Atp6ap2* in E12 embryonic cortex of *wild type* (WT) and *cKO* mice. VZ: ventricular zone. Dotted lines: ventricular surface, Scale bars: 10 μ m. (B) *Pals1* immunostaining at cortical-subcortical boundary at E12. The reduced expression of *Pals1* is restricted to the dorsal cortex (VZ) comprising the area of conditional *Atp6ap2* deletion in *cKO*s, in ganglionic eminences (GE) in mutants *Pals1* is normal. Scale bars: 50 μ m. (C) S-phase cells transiently labelled by BrdU and M-phase cells stained with Ki67 are significantly reduced in *cKO*. BrdU/Ki67 double-staining following BrdU pulse labelling 24 h earlier show increase rate of cell cycle exit in *cKO* indicated by reduced ratio of BrdU+/Ki67+ double positive cells. Dotted lines: ventricular surface, Scale bars: 50 μ m. Graph: Individual values and Mean \pm SEM. n=6 sections from 3 different litters. *** P <0.001, Student's t-test (unpaired, two-tailed). (D) Double immunostaining Tuj1 and activated caspase3 shows pronounced cell death of young neurons. Scale bars: 100 μ m.

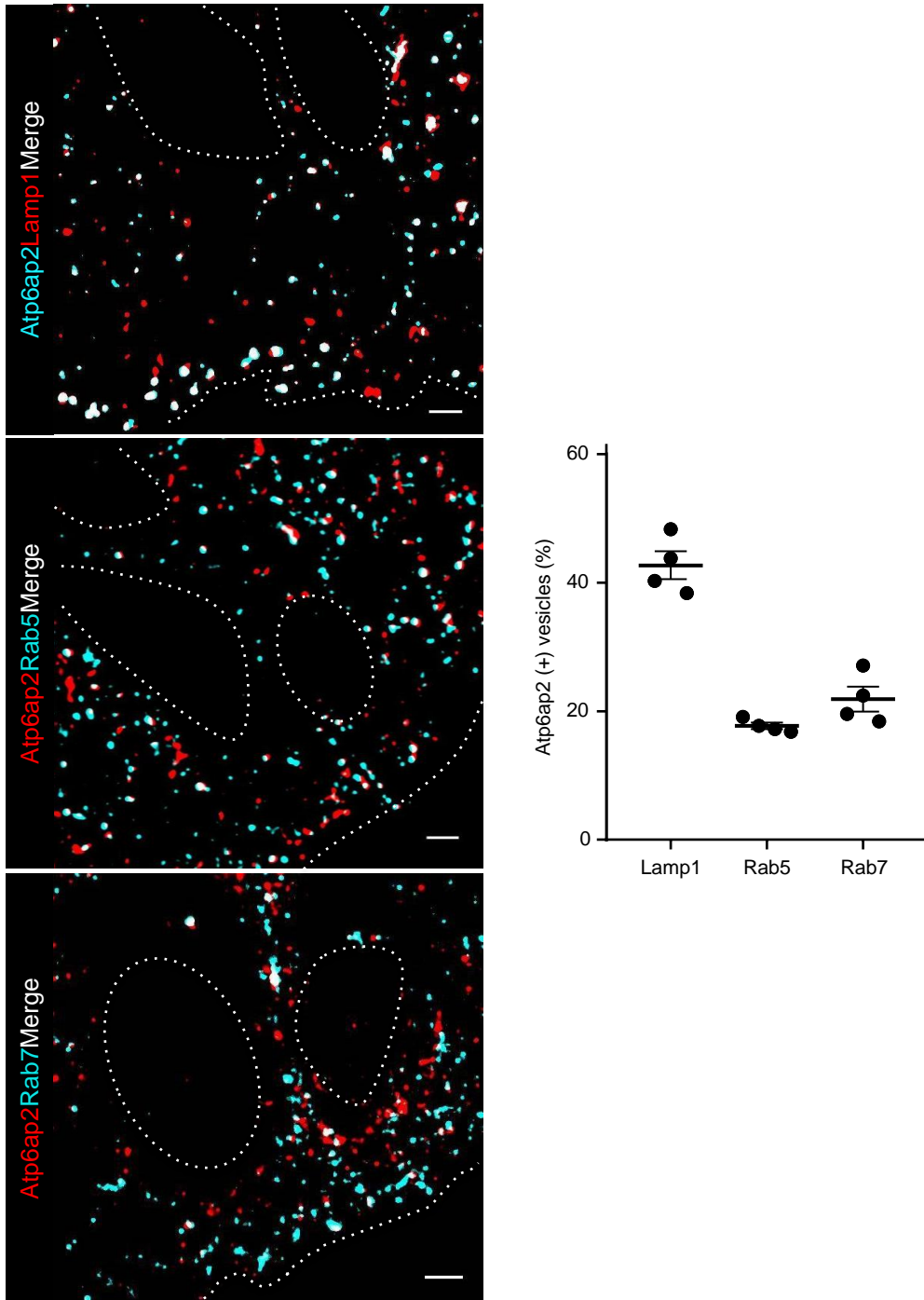
A



B

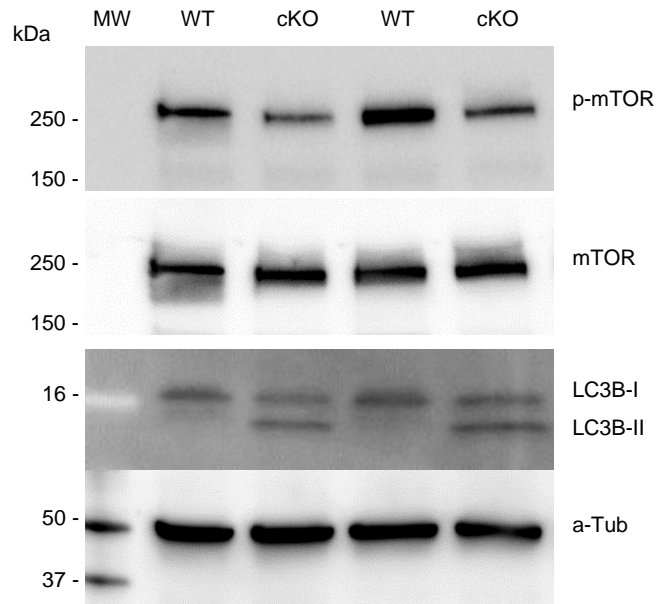


Supplemental Figure 2. Western blots of E12 cortex tissue. (A) Reduction of apical complex and adherens junction proteins in E12 cKOs. (B) Quantification of Western blots. Data shows individual values and Mean \pm SEM. n=3 different animals/group. ** P <0.01; *** P <0.001, Student's t-test (unpaired, two tailed).

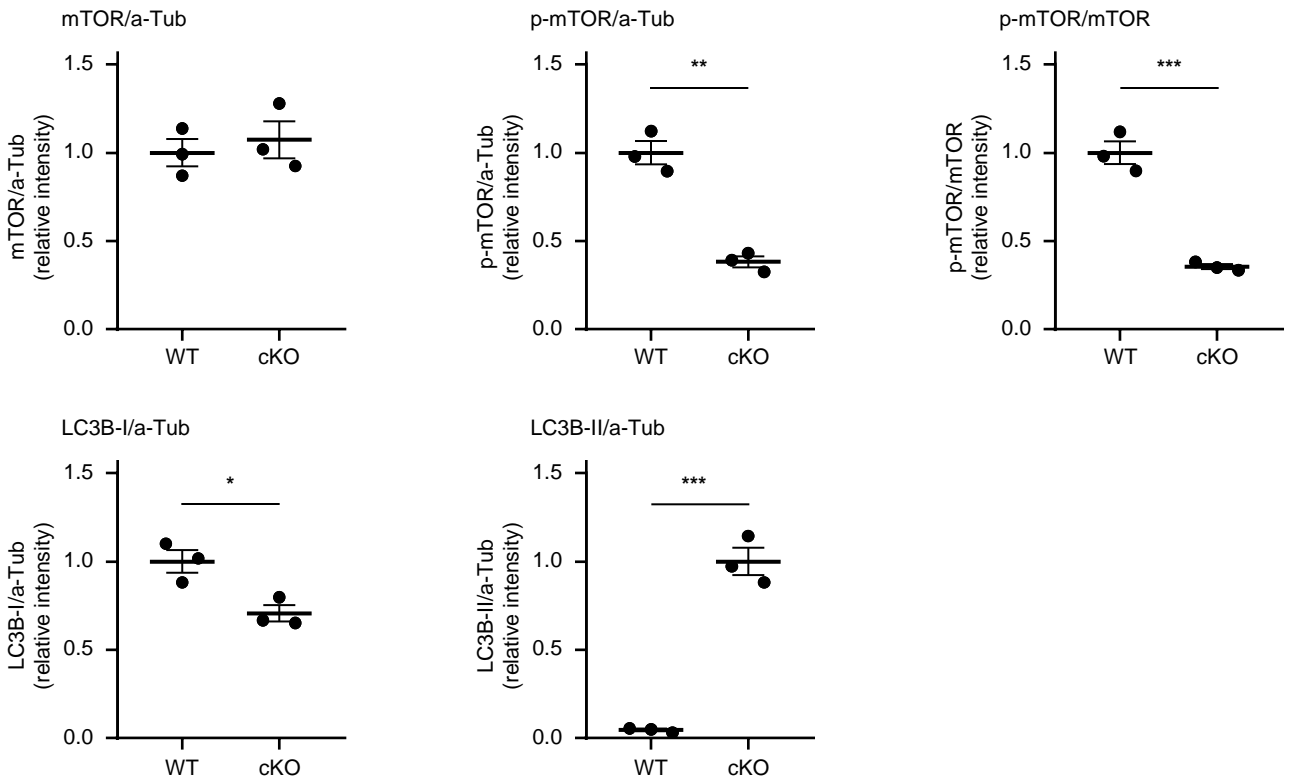


Supplemental Figure 3. Subcellular localization of Atp6ap2 in E12 radial glial cells analyzed by super-resolution Stimulated Emission Depletion (STED) imaging. Cortices from *wild type* E12 were stained with anti-Atp6ap2, anti-Lamp1, anti-Rab5 and anti-Rab7 and analyzed by STED. Atp6ap2 is largely undetectable at the plasma membrane and predominantly found in intracellular vesicles, lysosomes, early and late endosomes stained with anti-Lamp1, anti-Rab5 and anti-Rab7, respectively. Dotted lines: ventricular surface and nuclei, Scale bars: 1.0 μ m. Graph displays the percentage of double positive vesicles (individual values and Mean \pm SEM). n=4 sections from 2 different litters.

A

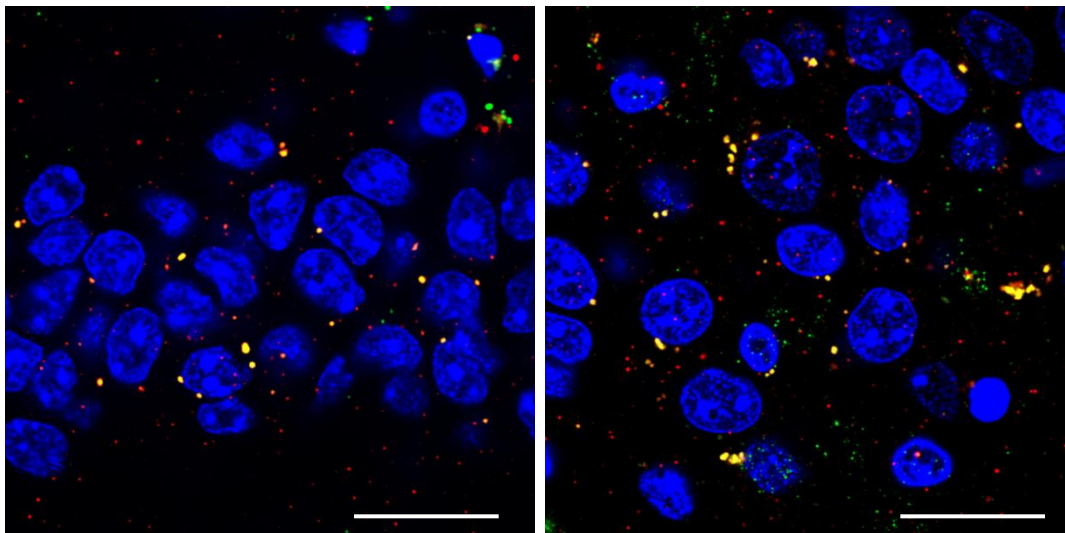


B



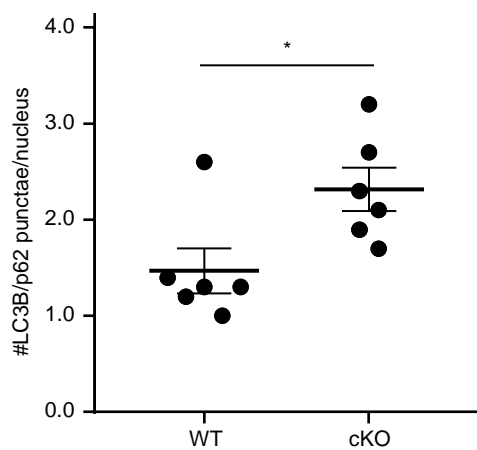
Supplemental Figure 4. Western blots of E12 cortex tissue. (A) Reduction of phospho-mTOR and increased LC3B-II in cKOs. (B) Quantification of Western blots. Data shows individual values and Mean \pm SEM. $n=3$ different animals/group. * $P<0.05$; ** $P<0.01$; *** $P<0.001$, Student's t-test (unpaired, two tailed).

p62 LC3B DAPI

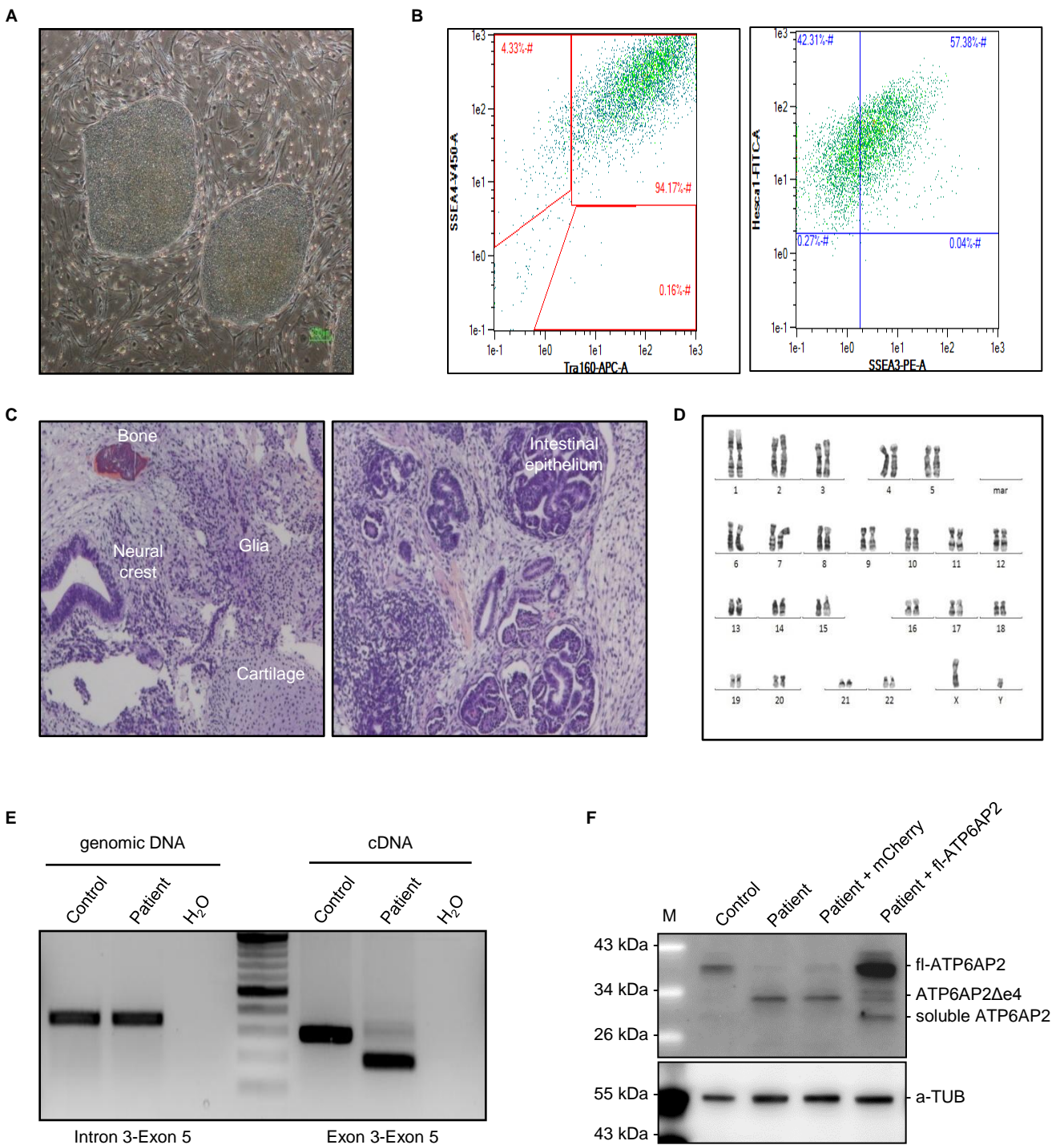


WT

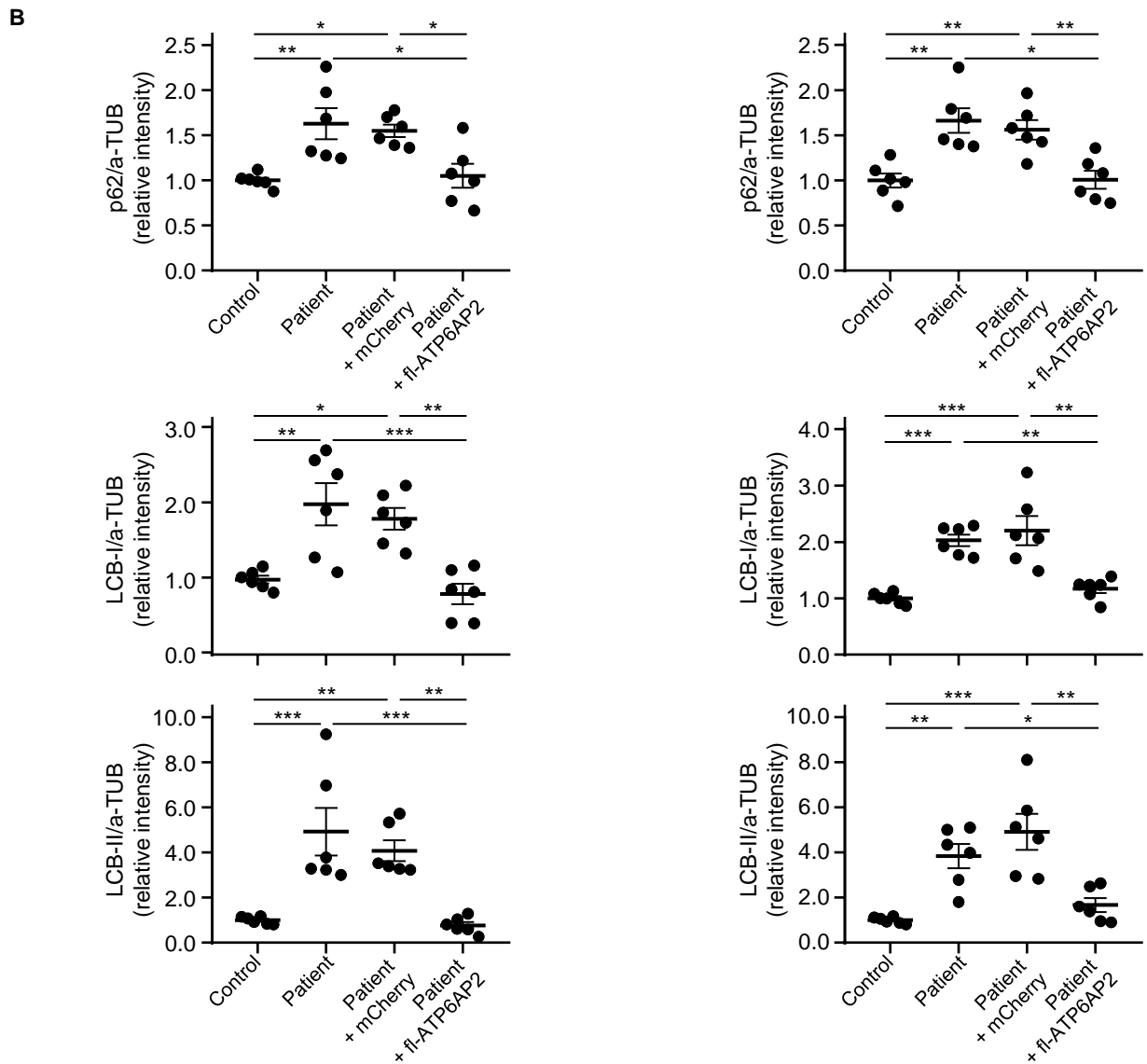
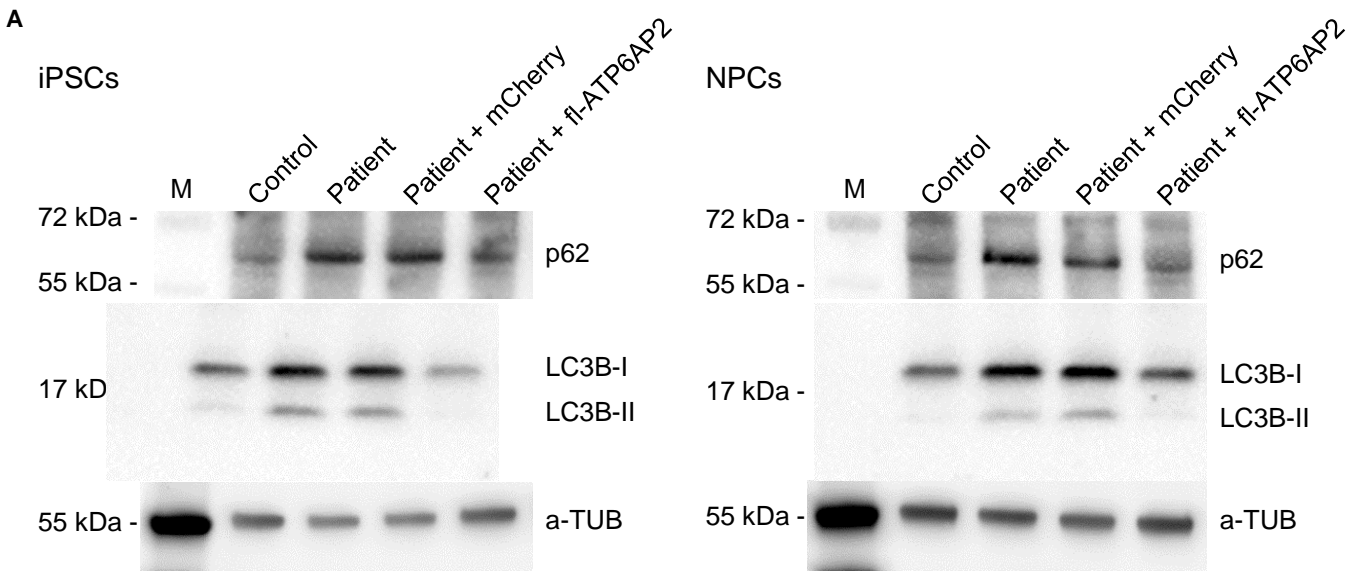
cKO



Supplemental Figure 5. Postnatal *Atp6ap2* deletion in postmitotic neurons. Immunostaining in *cKO*s shows enlarged lysosomes and accumulation of LC3B and p62 double positive aggregates in the hippocampus (CA1). Data shows individual values and Mean ± SEM. n=6 different animals/group. * $P < 0.05$, Student's t-test (unpaired, two tailed). Scale bars: 20 μ m.

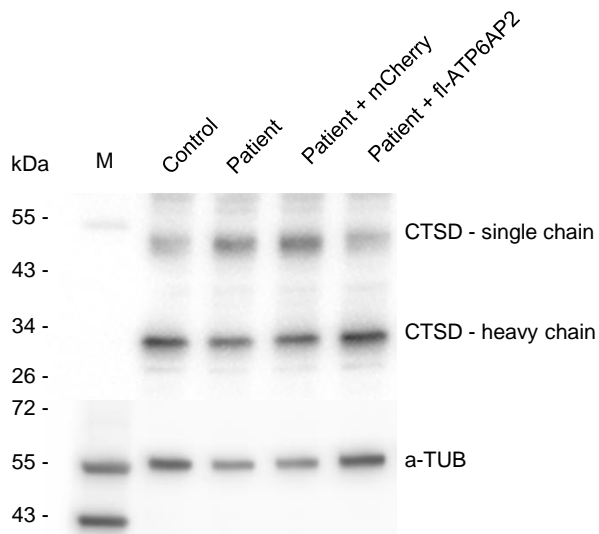


Supplemental Figure 6. Generation of iPSCs and assessment of pluripotency. (A) Morphology of iPSC clones generated from the patient carrying *ATP6AP2* [c.301-11_301-10delTT] variant. (B) Flow cytometry analysis of co-expression of stem-cell-specific surface proteins SSEA4, TRA-1-60 and SSEA3 and stem cell antigen human early stem cell antigen-1 (HESCA-1). (C) Hematoxylin/eosin staining of teratomas derived from patient iPSC showing generation of tissues derived from all germ layers. (D) Normal karyotype of patient derived iPSC line. (E) PCR analysis of the patient iPSCs using primers in intron 3 and exon 5 for genomic DNA and in exon 3 and exon 5 for cDNA. (F) ATP6AP2 Western blot of iPSC lines. The patient cell lines (with or without lentiviral vector control expressing mCherry) expressing the ATP6AP2Δ4 protein product. The cell line 'patient + fl-ATP6AP2' carries a lentiviral vector for the re-expression of full-length ATP6AP2.

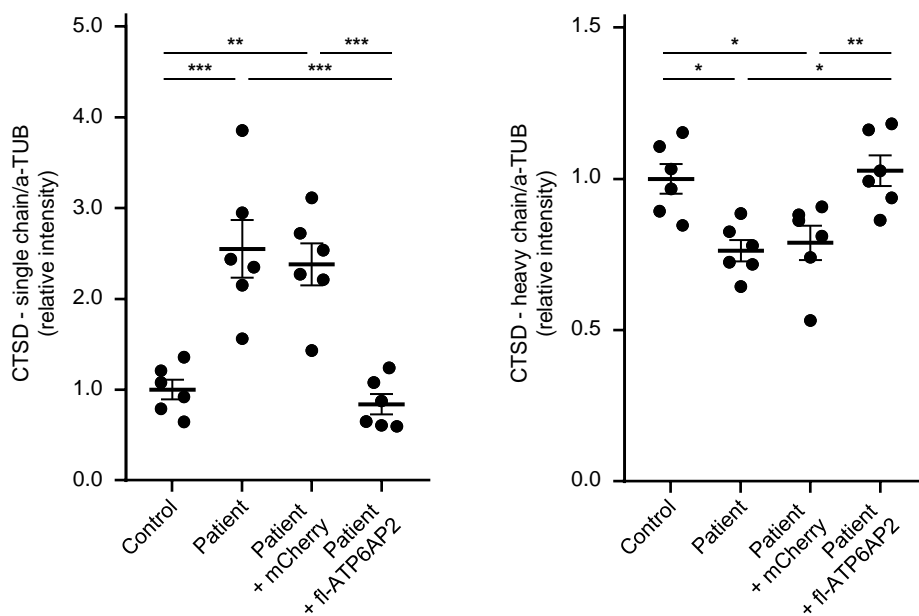


Supplemental Figure 7. Western blots iPSCs and neural progenitor cells (NPCs). (A) Increased p62 and LC3B in patient lines is rescued by re-expression of fl-ATP6AP2. (B) Quantification of Western blots. Data shows individual values and Mean \pm SEM. $n=6/\text{group}$. * $P<0.05$; ** $P<0.01$; *** $P<0.001$, one-way ANOVA followed by Bonferroni post-test.

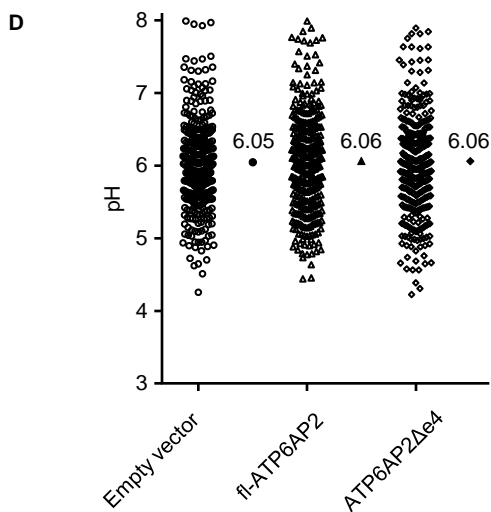
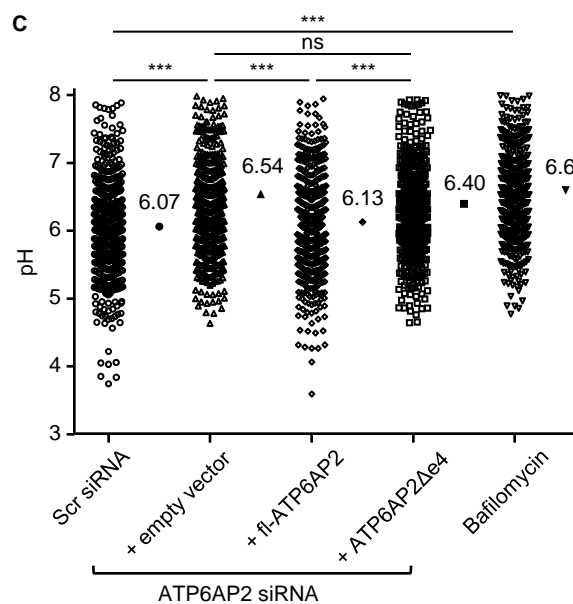
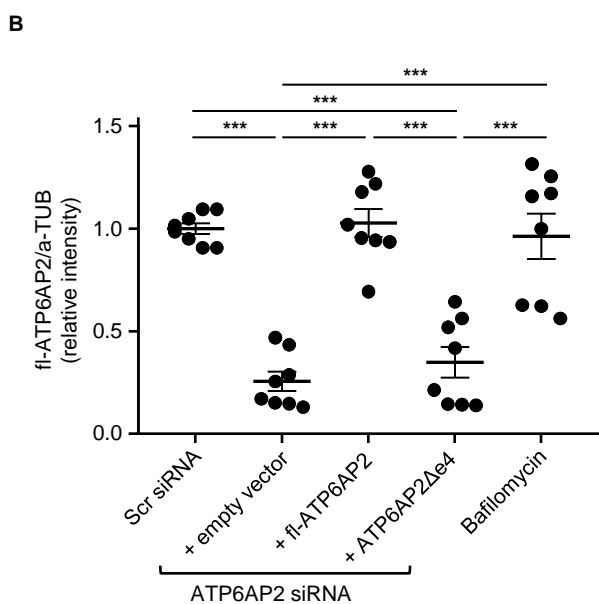
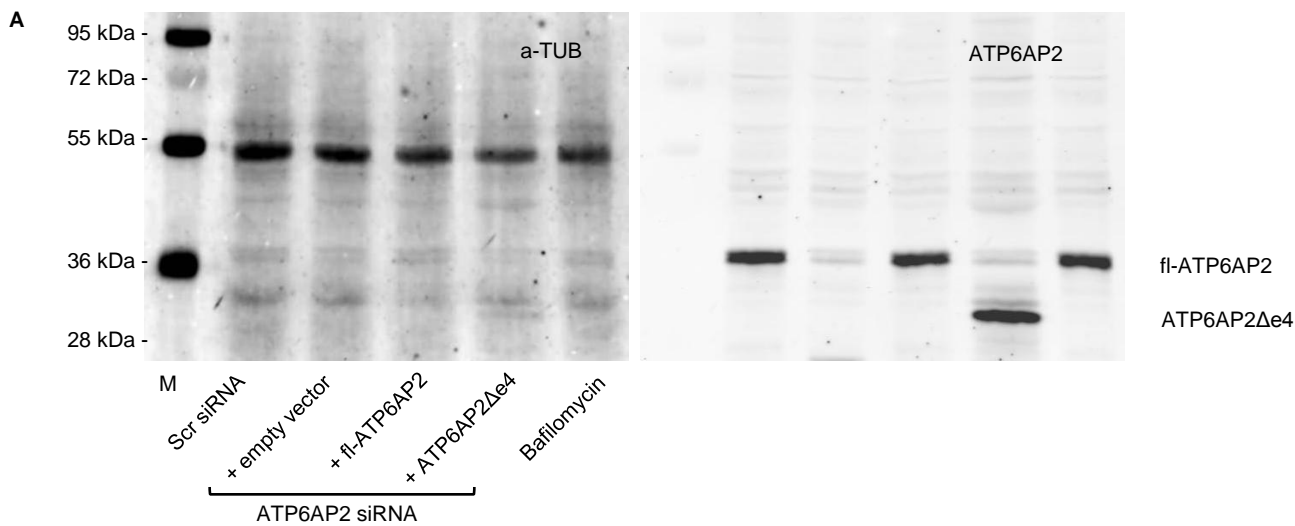
A



B

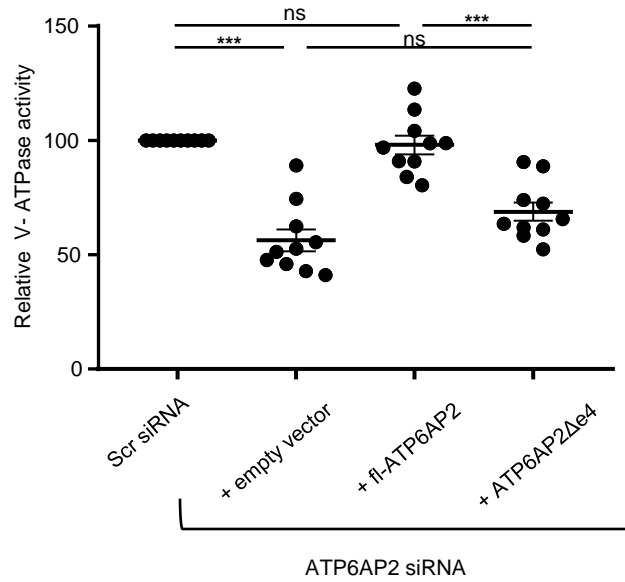


Supplemental Figure 8. Western blots of iPSC-derived neural progenitor cells (NPCs). (A) Impaired CathepsinD (CSTD) processing in patient lines is rescued by re-expression of fl-ATP6AP2. (B) Quantification of Western blots. Data shows individual values and Mean \pm SEM. $n=6$ /group. * $P<0.05$, ** $P<0.01$, *** $P<0.001$, one-way ANOVA followed by Bonferroni post-test.

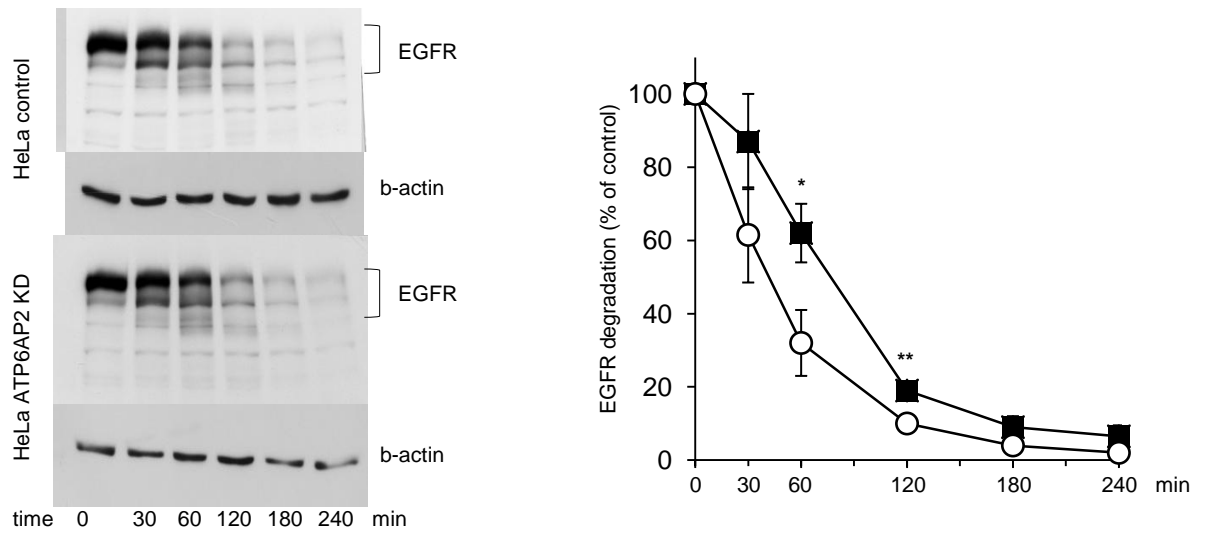


Supplemental Figure 9. ATP6AP2 siRNA knockdown in HeLa cells impairs vesicular acidification.

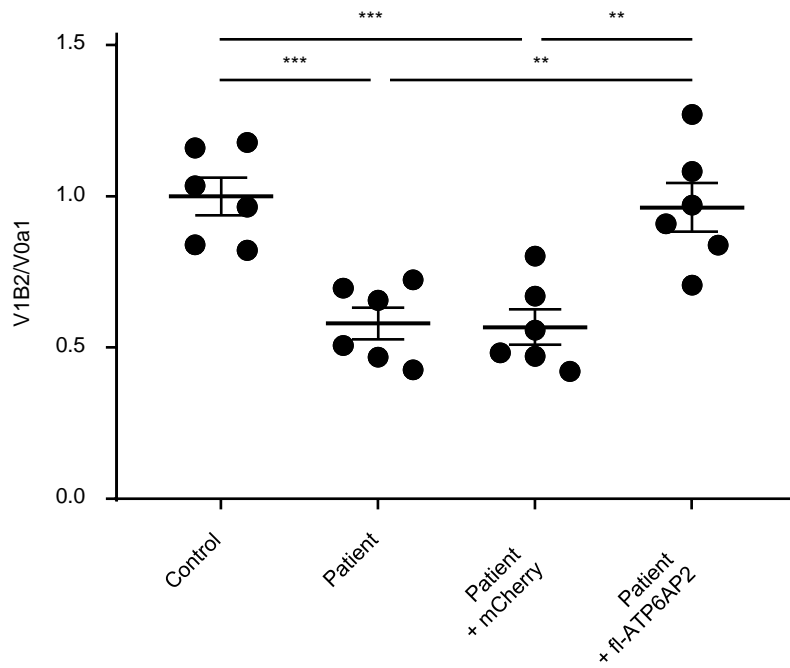
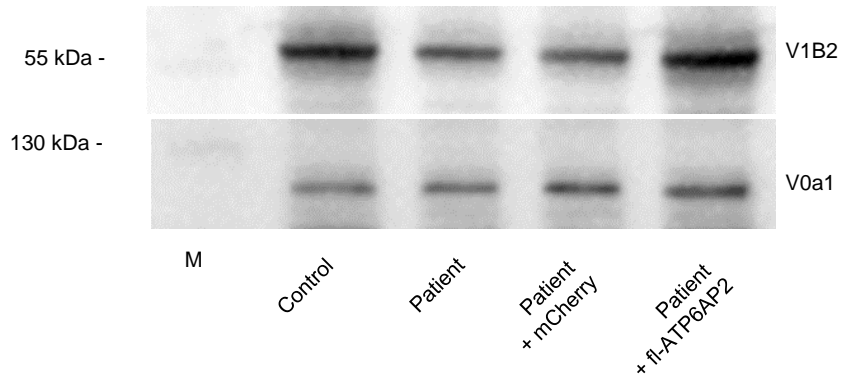
(A) HeLa cells were transfected with scramble (Scr) siRNA, 3'-UTR ATP6AP2 siRNA, or co-express 3'-UTR ATP6AP2 siRNA and fl-ATP6AP2 or co-express 3'-UTR ATP6AP2 siRNA and ATP6AP2Δe4, or treated with proton pump inhibitor bafilomycin. Cell lysate was analyzed by Western blot 24 h post transfection. Left: a-Tubulin loading control with molecular weight marker (M). Right: ATP6AP2. (B) Quantification of Western blots. Data shows individual values and Mean±SEM. n=8/group from four different experiments. *** $P < 0.001$, one-way ANOVA followed by Bonferroni post-test. (C) Vesicular pH in HeLa cells transfected with Scr siRNA or ATP6AP2 siRNA with or without fl-ATP6AP2 and ATP6AP2Δe4, or cells treated with bafilomycin. Graph shows individual vesicular pH and the median value. n=436-553 measurements from five independent experiments. *** $P < 0.001$; ns: $P > 0.05$, Kruskal-Wallis test (chi-squared=174.42, df=4, $P < 0.001$) followed by Dunn's multiple comparison test. (D) Overexpression of fl-ATP6AP2 or ATP6AP2Δe4 does not change vesicular pH. Graph shows individual vesicular pH and the median value. n=366-386 measurements from two independent experiments. Kruskal-Wallis test (chi-squared=0.47, df=2, $P = 0.79$).



Supplemental Figure 10. *ATP6AP2* siRNA knockdown impairs lysosomal V-ATPase activity. HEK293T cells were transfected with scramble (Scr) siRNA, 3'-UTR *ATP6AP2* siRNA, or co-express 3'-UTR *ATP6AP2* siRNA and fl-*ATP6AP2* or co-express 3'-UTR *ATP6AP2* siRNA and *ATP6AP2*Δe4. Cells were analyzed 48 h post transfection. Scr siRNA serves as reference, defining 100% in each experiment. n=10/group, one-way ANOVA $F(3, 36)=33.8383$, *** $P<0.001$ by Bonferroni post-test.



Supplemental Figure 11. *ATP6AP2* siRNA knockdown in HeLa cells impairs epidermal growth factor receptor (EGFR) degradation. HeLa Silencix cells stably expressing *ATP6AP2* shRNA or scramble shRNA were incubated with recombinant human EGF and cell lysate was analyzed at 0, 30, 60, 120, 180, 240 minutes. Left: Representative Western blot. Right: Quantification of the blots. Data shows Mean \pm SEM. n=3/group from three independent experiments. * P <0.05; ** P <0.01, Mann Whitney U test.



Supplemental Figure 12. Western blots of iPSC-derived neural progenitor cells (NPCs). Membrane-bound V1B2 subunit of the V1 sector and V0a1 subunit of the V0 sector of the V-ATPase of were analyzed by Western blot in iPSC-derived NPCs. Quantified as ratio of V1B2 to V0a1. Data shows individual values and Mean ± SEM. n=6/group. ** $P < 0.01$; *** $P < 0.001$, one-way ANOVA followed by Bonferroni post-test.